

MORPHOLOGY OF $Z \sim 1$ GALAXIES FROM DEEP K-BAND AO IMAGING

M. Huertas-Company¹, D. Rouan¹, G. Soucail², O. Le Fèvre³ and L. Tasca³

Abstract. We present the results of observations of distant galaxies ($z \sim 0.8$) at high spatial resolution ($\sim 0.1''$) aiming at studying their morphological evolution. We observed 7 fields of $1' \times 1'$ with the NACO Adaptive Optics system (VLT) in Ks ($2.2\mu m$) band with typical $V \sim 14$ guide stars and 3h integration time per field. The K-band has the key advantage to probe old stellar populations at these redshifts, enabling to determine galaxy morphological types unaffected by recent star formation, better linked to the underlying mass than classical optical morphology studies (HST). Observed fields are selected within the COSMOS survey area, in which multi-wavelength photometric and spectroscopic observations are ongoing. We analyze the morphologies by means of B/D (Bulge/Disk) decomposition with GIM2D and CAS (Concentration-Asymmetry) estimators for 79 galaxies with magnitudes between $K_s = 17 - 23$ and classify them in three main morphological types (Late Type, Early Type and Irregulars). We obtain for the first time an estimate of the distribution of galaxy types at redshift $z \sim 1$ as measured from the near infrared at high spatial resolution.

1 Introduction

The process of galaxy formation and the way galaxies evolve is still one of the most important unresolved problems in modern astrophysics. In the currently popular hierarchical picture of structure formation, galaxies are thought to be embedded in massive dark halos that grow from density fluctuations in the early universe and initially contain baryons in a hot gaseous phase. This gas subsequently cools, and some fraction eventually condenses into stars. However, many of the physical details remain uncertain, in particular the process and history of mass assembly. One classical observational way to test those models is classifying galaxies according to morphological criteria defined in the nearby Universe that can be related to physical properties and to follow this classification across time. Progress in this field has been coming from observing deeper and larger samples, but also from obtaining higher spatial resolution at a given flux and at a given redshift. In the visible, progress has been simultaneous on those two fronts, thanks to the ultra-deep HDF fields observed with Hubble Space Telescope. In particular, HST imaging has revealed observational evidence that galaxy evolution is differentiated with respect to morphological type. In this context, near infrared observations are particularly important because the K band flux is less dependent on the recent history of star formation, which peaks in the UV in rest frame, and gives thus a galaxy type from the distribution of old stars, more closely related to the underlying total mass than optical observations. This is why a large number of K-band surveys have been carried out using ground-based telescopes in order to perform cosmological tests by means of galaxy counts essentially. However, no morphological information can be found due, in particular, to the seeing limited resolution. Adaptive optics (AO) installed on ground based telescopes seems the only way today to obtain near-infrared high resolution data. The mean obtained spatial resolution of $0.1''$ with AO, which is better than the one ($0.2''$) obtained with HST NICMOS in the same band, permits a clear separation between exponential and de Vaucouleurs profiles at $z \sim 1$, despite limitations, inherent to AO, such as the non-stationary PSF on long integration times and the finite isoplanetic field. This is why preliminary studies to probe the accuracy of adaptive optics are required, before launching larger observations. In particular, it is important to determine whether automated morphological classifications can be performed. Minowa et al. (2005) used for the first time

¹ LESIA-Paris Observatory, 5 Place Jules Janssen, 92195 Meudon - France

² Laboratoire d'Astrophysique de Toulouse-Tarbes, 14 Avenue Belin, 31400 Toulouse, France

³ LAM-Marseille Observatory, Traverse du Siphon-Les trois Lucs BP8-13376 Marseille Cedex 12 -France

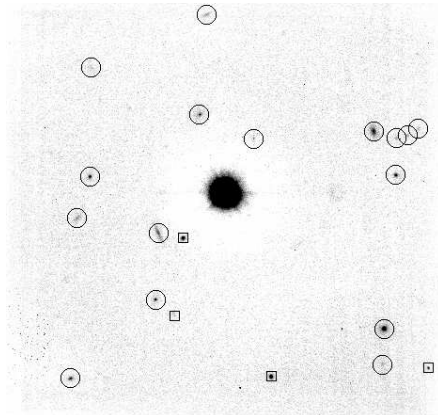


Fig. 1. NAOS/CONICA K_s -band image of the field centered at $\alpha = 10:00:16$, $\delta = +02:16:22$. The total integration time is 10350s. The field size is $1' \times 1'$ with a pixel scale of $54mas$. Circles are detected galaxies and boxes are stars. The stellar FWHM was measured to be $0.1''$. The bright star at the center of the image was used as the AO guide star.

adaptive optics for those purposes. They achieved a limiting magnitude of $K \sim 24.7$ with the Subaru Adaptive Optics system with a total integration time of $26.8hr$ over one single field of $1' \times 1'$. They proved that the use of adaptive optics significantly improves detection of faint sources but did not obtain morphological information. In a more recently submitted paper, Cresci et al. (2006) performed a morphological analysis with AO data for the first time. They observed a 15 arcmin^2 in the K_s band with NACO (SWAN survey) and classified distant galaxies into two morphological bins (late type and early type) by performing a model fitting with a Sersic law. They compared number counts and size-magnitude relation for early and late-type separately with hierarchical and Pure Luminosity Evolution (PLE) models respectively. However, as discussed in several studies (i.e. Gardner 1998), despite that galaxy counts are still one of the classical cosmological tests, their interpretation remains difficult. It is not thus realistic to expect galaxy counts alone to strongly constrain the cosmological geometry or even to constrain galaxy evolution. A more complete study needs redshift estimates, which is lacking in the SWAN survey. That's the main reason why our pilot programme has been selected within the on-going Cosmic Evolution Survey (COSMOS, Scoville et al. 2005) in which multi-wavelength photometric and spectroscopic observations are performed. This ensures a reliable redshift estimate for all our objects. In this paper, we continue this AO validation task by morphologically classifying a sample of 79 galaxies, using parametric (GIM2D, Simard et al. 2002) and non-parametric (C-A, Abraham et al. 1994) methods and comparing them. Fields, observed with the NAOS/CONICA adaptive optics system, are distributed over a 7 arcmin^2 area. By the way, we obtain for the first time an estimate of the distribution of galaxies in three morphological types (E/S0,S,Irr) at redshift $z \sim 1$ as measured from the near infrared at high spatial resolution. In a submitted paper, we use the known photometric redshifts to look for evolution indices as a function of morphology.

2 The Data Set

7 fields of $1 \text{ arcmin} \times 1 \text{ arcmin}$ were observed with the NAOS/CONICA adaptive optics system installed on the VLT, in the near-infrared (K_s band, $2.2\mu\text{m}$)¹. The fields were selected within the COSMOS survey area². In order to ensure a reliable AO correction, relatively bright stars ($V \sim 14$) were selected. The pixel scale (0.054 arcsec) was chosen to be twice the Shannon requirements at the telescope diffraction limits in order to have larger fields to perform statistical analysis and better sensitivity. Indeed, this program represents a technical challenge since the limits of adaptive optics are practically reached: wide field observations with long exposure times and a guide star not bright enough for a full AO correction. We find 285 objects over the 7 fields.

¹P73.A-0814A and P75.A-0569A

²<http://www.astro.caltech.edu/cosmos/>

We then performed a cleaning task in order to separate galaxies from stars and spurious detections. This was made using the SETRACTOR MU_MAX and MAG_AUTO parameters that give the peak surface brightness above background and the Kron-like elliptical aperture magnitude respectively. Distribution of objects in this parameter space clearly defines three regions that easily separate extended sources from point-like or non-resolved sources and from spurious detections. We consequently identify 79 galaxies, 19 stars (or unresolved objects) and 187 spurious objects in the whole 7 fields.

The sample completeness for point sources is estimated by creating artificial point sources from fields stars. We find that the sample is 50% complete at $K_s = 22.5$ (or $AB = 24.5$) for point sources and at $K_s = 21.5$ (or $AB = 23.5$) for extended sources.

3 Photometric redshifts

NACO fields are selected within the on-going COSMOS survey in which multi- λ and spectroscopic observations are performed. In addition, these fields are observed at CFHT (MEGACAM) in 5 photometric bands (u^*, g', r', i', z') from the near-UV to visible domain. All these data were used for a direct estimate of the photometric redshifts of the galaxies detected in the NACO fields, computed with the code *LePhare*³. This method allows to reach an accuracy $\sigma_{\Delta z}/(1+z_s) = 0.031$ with $\eta = 1.0\%$ of catastrophic errors, defined as $\Delta z/(1+z_s) > 0.15$. As expected the redshift distribution is centered around 0.8 (Mignoli et al. 2005).

4 Automated Morphological Classifications

The 79 objects identified as extended sources have been morphologically classified using two automated methods based on direct model fitting and on learning classification respectively.

4.1 Irregular objects

The detection of objects presenting irregularities was made using the concentration and asymmetry estimators. We thus simulated a set of galaxies with different galactic parameters and magnitudes ranging between $17 < K_s < 23$ that we embedded in the real images. We computed the C and A parameters of these objects and represented the C-A plane. Since irregular objects cannot be simulated in a meaningful way, a kind of extrapolation was employed, based on two facts: a)irregular galaxies are supposed to have flatter photometric profiles (less concentrated) and to be more asymmetric than regular objects; b)those objects are not present in the simulated sample. We thus defined the irregular zone as the upper left corner of the C-A plane where no simulated objects are found.

4.2 Regular Objects

4.2.1 CAS morphology

The border between early and late type objects can be deduced in a more automated way thanks to the analysis of simulated galaxies. We took the same 500 galaxies as above, for which the morphological type is known and draw their positions in the C-A plane. The border was then defined with a classification method based on Support Vector Machines⁴.

4.2.2 Model Fitting Morphology

The second method is based on a direct two components fitting with exponential and de Vaucouleurs profiles, using GIM2D. In order to obtain reliable results, GIM2D needs a noise-free, well-sampled PSF. This is why special attention has been paid to PSF reconstruction. Indeed, classical methods such as DAOPHOT or Tiny Tim could not be used because of two main reasons: first, the Adaptive Optics PSF has a specific shape which is neither 'seeing limited like' nor 'spatial like'. We developed a simple algorithm that uses field stars to generate Shannon sampled PSFs by means of a fitting procedure in the Fourier Space. Working in the Fourier Space

³http://www.lam.oamp.fr/arnouts/LE_PHARE.html

⁴<http://www.isis.ecs.soton.ac.uk/resources/svminfo/>

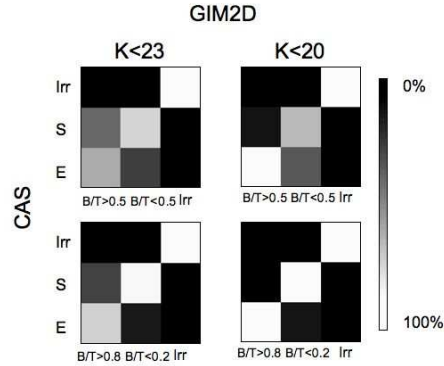


Fig. 2. Comparison of classification methods. The figure shows the probability that a galaxy classified with GIM2D is classified in the same morphological type by CAS. (see text for details).

avoids including the background estimate and PSF position as a fit parameter, which is particularly delicate in our case, since the FWHM is less than 2 pixels large. We run GIM2D on the 79 objects with magnitudes ranging between $K_s = 17 - 22$ using a two components model and with the artificial PSF built as described above. The fitting converged for the whole sample, and the results are quite convincing in terms of residual images.

4.3 Results of the analysis and comparison of classifications

We classified the galaxies into three main morphological types according to the fitting results. One of the main results is that about 25% of our sample corresponds to peculiar or irregular objects (19 objects out of 79). For the rest of the sample, the GIM2D analysis gives about 25% of bulge dominated galaxies ($B/T > 0.5$) and 53% of disk dominated ($B/T < 0.5$) while for the CAS classification, we find 40% of spiral galaxies and 20% of elliptical ones. We also computed the probability that a galaxy classified using the GIM2D classification is classified with the same morphological type by CAS. The probability has been computed by dividing the number of galaxies in each morphological CAS bin by the total number of galaxies of the same type selected with GIM2D. Overall, there is a good agreement between both classifications in the whole sample: the probability that a spiral galaxy identified by GIM2D has the same morphological type in CAS classification is $p = 0.75$ and $p = 0.65$ for early type galaxies including the faintest objects ($K_s < 23$). For irregulars it is obviously $p = 1$ since the detection procedure is the same in both methods.

There might be two reasons why the classifications are not exactly the same: First, the S/N ratio might cause discrepancies. Indeed at low S/N ratio GIM2D tends to under-estimate the bulge fraction. This implies that galaxies detected by GIM2D as disk dominated are in fact detected as early type by CAS. Fig. 2 shows the effect of reducing the limiting magnitude to $K_s = 20$: the fraction of objects classified as bulge dominated by GIM2D and CAS rises up to 0.85. Second, it might be a problem of definition. Indeed, the morphological bins are not exactly the same in both classifications. In particular, objects with intermediate morphological type (i.e $B/T \sim 0.5$) might cause discrepancies. If we remove those objects from the sample all the early type objects and 90% of the late type objects detected by GIM2D are also detected by CAS with the same classification. This gives for the first time an estimate of the galactic population at $z \sim 1$ in the near infrared at high spatial resolution. We confirm thus a well known result: the fraction of perturbed objects increases with redshift. However this result must be taken with caution. Indeed GIM2D accuracy falls for objects fainter than $K_s = 19$, which represents 80% of the sample. Moreover at the faint end, the fraction of irregular objects can be over estimated because of the low signal-to-noise ratio. In addition there can be a mismatch between local and high redshift morphological classifications due to the “morphological k-correction”. But there are good reasons to consider this result significant: even though there is an over estimation of disks in the faint end, the morphological classification bins are large enough to reduce the number of false classifications. Indeed, even in the zones where the random error in the bulge fraction estimate is ~ 0.3 or larger we will not classify a pure

bulge ($B/T \sim 1$) as a disk.

5 Summary and Conclusions

We analyzed the morphologies of a sample of 79 galaxies in the near-infrared thanks to adaptive optics imaging at a resolution of $0.1''$. We showed that adaptive optics can be used to obtain reliable high resolution morphological information in an automated way, and is thus adapted to larger observation programs. We obtained, for the first time an estimate of the galactic population in the near-infrared at $z \sim 1$. In a submitted paper (Huertas-Company et al. 2006) we combine the redshift estimates to obtain a rough redshift distribution for each morphological type and compare it to HST-ACS imaging.

References

- Abraham, R., Valdes, F., Yee, H.K.C., van den Bergh, S. 1994, ApJ, 432, 75
Cresci, G., Davies, R., Baker A.J., et al. 2006, arXiv:astro-ph/0607221
Gardner, J. 1998, PASP, 110, 291
Mignoli, M., Cimatti, A., Zamorani, G., et al. 2005, A&A, 437, 883
Minowa, Y., Kobayashi, N., Yoshii, Y., et al. 2005, ApJ, 629, 29
Scoville, N., & COSMOS Team 2005, BAAS, 1309
Simard, L., Wilmer, C., Vogt, N.P., et al. 2002, ApJS, 142, 1